Journal of New Technology and Materials (JNTM)
J. New Technol. Mater.
Vol. 09, N°01 (2019)28-35

OEB Univ. Publish. Co.

Growth and properties of SnO_2 thin films obtained by spray pyrolysis technique

B. Bendahmane*, N. H. Touidjen, and F. Mansour

Laboratory of Study of Electronic Materials for Medical Application (LEMEAMED), Electronic department, Sciences and Technology faculty. Freres Mentouri University, Constantine, 25000, Algeria.

*Corresponding author, email: bendahmane.boutheina92@gmail.com

Received date: March 18, 2019 ; accepted date: Apr. 21, 2019

Abstract

SnO_2 (Tin oxide) metal oxide is considered as one of the most investigated II-VI semiconductor in modern microelectronic technology. Several techniques have been used to deposit SnO_2 thin films. Among them, spray pyrolysis has proved to be simple, inexpensive and allows the control of many films parameters. In this work, various parameters of the spray pyrolysis technique are optimized to obtain SnO_2 thin films. The starting solution molarity M and the deposition temperature T_d are fixed at 0.075 M, 0.1 M and T_d=350°C, 400°C, respectively. To investigate the films properties, structural, morphological and optical characteristics using X-ray Diffractometry (XRD), Scanning Electron Microscopy (SEM), Energy-Dispersive X-ray Spectroscopy (EDX), Atomic Force Microscopy (AFM) and UV-Visible spectrophotometry are studied respectively. XRD measurements show that SnO_2 thin deposited films are polycrystalline with a typical tetragonal structure, except the 350°C-0.075 M film, which shows a beginning of crystallization. SEM and AFM micrographs reveal rough and porous films surfaces with an agglomeration effect of nanoparticles that do not exceed 20 nm. EDX analysis confirms the chemical composition of pure SnO_2. Optical characterization shows that absorption peaks decrease strongly from near UV to visible wavelength while a slow decrease of absorption is observed in the visible-IR range. Moreover, a large band gap E_g for all deposited films is estimated.

Keywords: Spray pyrolysis, SnO_2, XRD, SEM, AFM, UV-Vis.

1. Introduction

Since the last decade, there has been a great deal of interest in deposition of tin oxide SnO_2thin semiconductor films because of their wide applications in new technology such as chemical gas sensors [1, 2],electrodes in solar cells [3],anodes for lithium-ion batteries [4], and Schottky diodes [5]. A variety of processes and methods has been used to deposit thin films; these include physical vapor deposition (PVD) [6], laser molecular beam epitaxy [7], sputtering [8], chemical vapor deposition (CVD) [9], sol-gel [10], spin and dip-coating [11]. Among these techniques, spray pyrolysis is a simple and cost effective processing method. It is well suited for preparation of doped and undoped semiconductors thin films and provides optically smooth, uniform and homogeneous layers on various substrates depending on the deposition parameters [12, 13]. The preparation procedures and experimental conditions play important role enhancing the film properties.In a previous work [2], we have presented a detailed study of SnO_2 film deposited at T_d=400°C from ($SnCl_2$ $2H_2O$) solution with 0.1 M molarity. We showed that this film is suitable for chemical sensor application. In order to complete the investigation of SnO_2 thin films properties, we study in the present paper the effect of molarities and substrate temperatures on the films characteristics using the same experimental procedure, with 0.075 M, 0.1 M molarities and T_d=350°C, 400°C.

2. Experimental procedure

The schematic experimental equipment (HOLMARC, model HO-TH-04) of the spray pyrolysis technique available in our laboratory is shown in Figure 1. The spray pyrolysis system has been designed for laboratory researches in thin films field, especially for the development of microelectronic devices. Moreover, ergonomically designed chamber provides clean and healthy atmosphere suitable for modern laboratories conditions. Parameters like dispensing rate of the solution and speed of spray head movement are monitored by automatic system and the temperature of the substrate heater plate is controlled. The spray head movement is also controlled by stepper motor driven linear stages in X and Y directions. The temperature of the substrate heater plate is controlled by a chromel-alumel thermocouple. A desktop computer with windows OS is used to control the operations through serial port. Software programming for spray pyrolysis system can be used as well for documenting the relevant parameters used for solution preparation like temperature, air pressure, flow rate and duration. The different parameters used in the spray system and process deposition of SnO_2 thin films are listed in Table1.

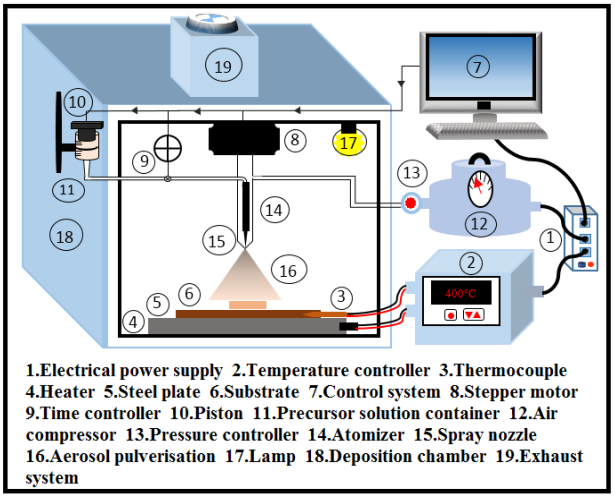

Figure 1. Schematic representation of the spray pyrolysis system.

Table1: Spray pyrolysis technical and optimized parameters for Holmarc equipment.

Spray pyrolysis parameters	
Technical parameters of Holmarc Equipment	Optimized deposition parameters in this work
Dispensing unit capacity : 250 ml & 500 ml	Solution concentration : 0.075 M & 0.1M Solvent : deionized water
Dispensing rate : 1-20ml/min	Solution flow rate : 0.5ml/min
Drive speed X axis : 10-800 mm/sec Drive speed Y axis : 1-12 mm/sec	Drive speed X axis : 10 mm/sec Drive speed Y axis : 10 mm/sec
Substrat base plate dimension : 150x150 mm Sprayer traverse : X-Y 200 mm max	Carrier gas : compressed air (2 bars)
Nozzle-substrate distance : 10-18 cm	Nozzle-substrate distance : 18 cm
Temperature maximum : 500°C	Substrate temperature : 350°C & 400°C

To obtain SnO_2 thin films, tin (II) dichloride dehydrate ($SnCl_2.2H_2O$, 99.8%, Aldrich) was used as precursor to achieve 0.075 M and 0.1 M. The starting solution was sprayed by the nozzle aerosol pulverization on glass substrate at two deposition temperatures T_d=350°C and 400°C, while deposition time was kept at 30 min. The other parameters, scanning nozzle speed, flow rate, distance nozzle-substrate, and gas pressure were fixed at 10 mm/s, 0.5 ml, 18cm, and 2 bars, respectively. These optimized parameters are based on several deposition conditions elaborated in our laboratory and compared to other works [14-17].

For the investigation of the crystalline structure, we used X-ray Diffractometer with CuKα radiation at λ=1.5418° and 2θin the range 20°-70°. Characterizations by Scanning Electron Microscopy (SEM), Energy-Dispersive X-ray Spectroscopy (EDX) and Atomic Force Microscopy (AFM) were employed to investigate morphology, chemical composition and topography of the deposited films, respectively. Optical parameters of the sprayed layers were measured using UV-Visible-IR spectrophotometer in the wavelength range 200nm-1500nm.

3. Results and discussion

3.1. Structural properties

Structural characteristics of SnO_2 thin films deposited on glass substrate were studied by XRD. Patterns represented in Figure 2 show a clear increase of peaks intensity with the molarity and deposition temperature T.

As indicated in Figure 2-a, for T_d=350°C and the molarity 0.075 M, we can see a beginning of crystallization in the layer revealed by one intense peak at 2θ=26.61° and no other significant peak. While XRD patterns obtained from samples deposited at 350°C and 400°C and both molarities 0.075 M and 0.1 M (Figs. 2-b, 2-c, and 2-d) indicate strong peaks corresponding to crystalline orientation (110) at 2θ=26.61°, and other less intense peaks according to (101) (200) and (211) planes at 2θ=33.9°, 37.99°, 51.82°, respectively. These peaks are the most intense given by JCPDS-ICDD card 041-1445 for tetragonal rutile structure of SnO2 phase. Deposition temperature has an important effect on the film formation and crystallization. For instance, at the low molarity 0.075 M films (Figs. 2-a and 2-b) the structure changed completely from a beginning of crystallization at 350°C to a complete polycrystalline phase at 400°C. While at the high molarity 0.1 M (Figs. 2-c and 2-d), both films are polycristalline, but the intensity of all peaks increased with the increase of deposition temperature from 350°C to 400°C especially the (200) and (220) peaks that are well identified at high temperature (T=400°C). This is similar to what was reported in [18], where A.A. Yadav et al. investigated the substrate temperature effect on SnO2 properties and they stated that high deposition temperature (T≥400°C) favors the chemical dissociation of the starting solution that leads to better crystallinity. Moreover, at high temperature T=400°C (figs. 2-b and 2-d), we notice that the (220) peak is more significant at the low molarity 0.075 M film (figure 2-b) then it disappears at high molarity 0.1 M (figure 2-d). These observations are confirmed by Nadir F. Habubi et al. work [17] where some peaks like (220) vanished with the increase of molarity; this may be due to the fact that at high temperature (T≥400°C), low solution concentration leads to faster and better crystallinity during the deposition process.

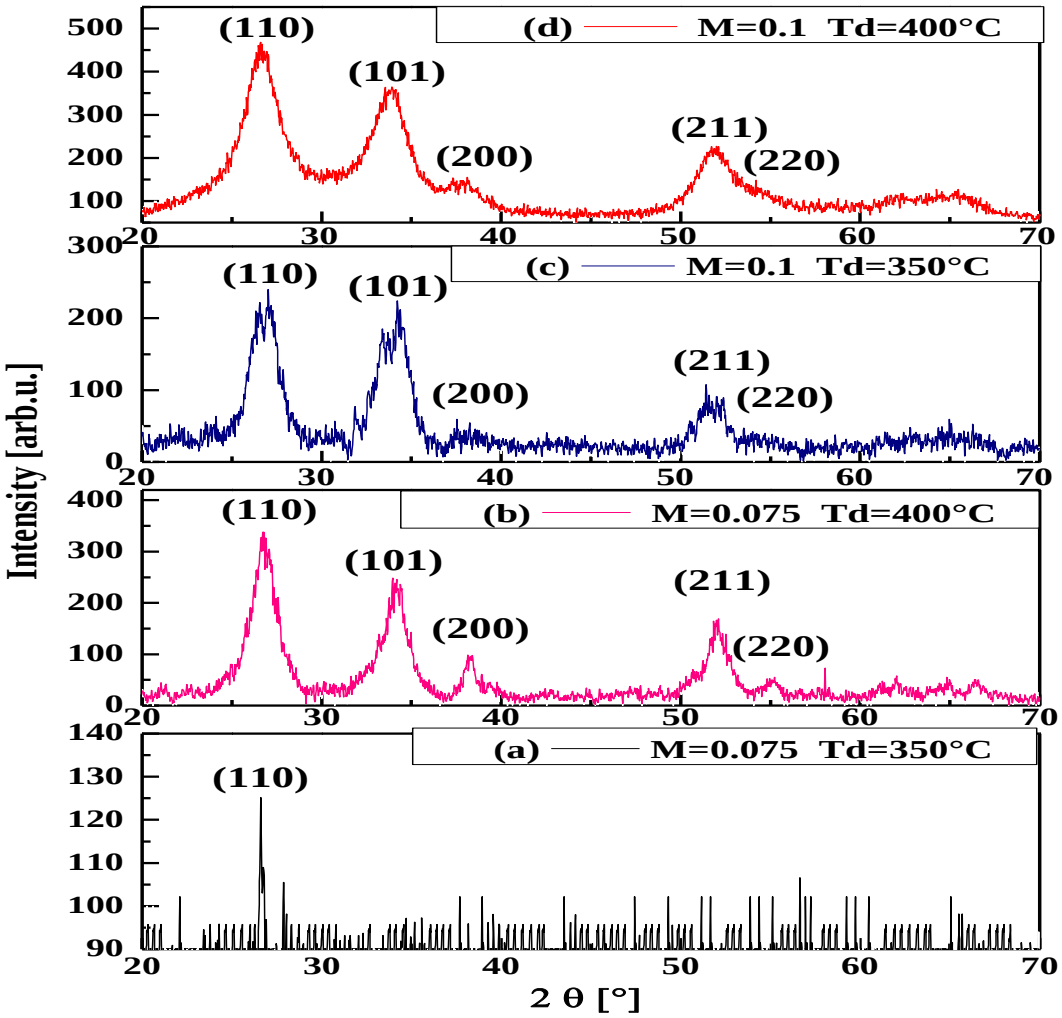

Figure 2. XRD patterns of SnO_2 sprayed thin films.

The average crystallites sizes D deduced from the patterns of the crystallized films (Figs 2-b, 2-c, and 2-d) are represented in Table 2. They are calculated using Scherrer's formula [19]:

$$D=0.9\lambda/(\beta\cos\theta)$$

Where λis the X-ray wavelength, βthe Full Width at Half Maximum (FWHM),and θthe Bragg angle.

The results listed in Table 2 indicate very small crystallites sizes D. This suggests that SnO_2 thin films structure reveals the presence of nanoparticles.

Table2: Crystallites sizes D of SnO_2 sprayed thin films.

Samples deposition parameters	D [nm]
(a) M=0.075 T_d=350°C	-
(b) M=0.075 T_d=400°C	10.30
(c) M=0.1 T_d=350°C	08.40
(d) M=0.1 T_d=400°C	17.47

3.2. Morphological characteristics

SEM observations of all deposited SnO_2samples presented in Figure 3 indicate rough and porous surfaces where grains and grains boundaries are randomly distributed with the presence of some cavities and pores. We observe in the four micrographs (Figs. 3-a, 3-b, 3-c and 3-d) that each grain is an agglomeration of a large number of crystallites or nanoparticles. The average grains sizes L are estimated in the range 500nm–800nm. These values are larger than the crystallites sizes (10nm–18nm) calculated from XRD.These results show that the observed grains are formed during the layers growth from an aggregation of nanoparticles. The same constatations have been reported in other works [20, 21].

Figure 4 presents EDX analysis carried out on SnO_2 sprayed films. At Td=350°C for both film molarities (Figs 4-a, 4-c and Table 3), the layer contains a mixture of tin (Sn), oxygen (O) and small amount of chlorine (Cl). While at higher temperature T_d=400°C, for 0.075 M and 0.1 M (Figs 4-b, 4-d), the element composition becomes a combination of tin (Sn) and oxygen (O) only, as shown also in Table 3. We can conclude that EDX atomic

percentage results confirm a good stoichiometry of most sprayed deposited films revealing pure SnO_2 layers and this is well correlated with XRD results discussed in section 3.1. However, we note that the film Td=350°C, 0.075 M (Fig 4-a) shows the presence of Si element coming from glass substrate that indicates a non-homogenous layer at these conditions as mentioned by G.S. Park et al. [22].

Table 3: Chemical composition of tin oxide sprayed thin films obtained by EDX analysis.

Element	(a) M=0.075 T_d=350°C (Atom %)	(b) M=0.075 T_d=400°C (Atom %)	(c) M=0.1 T_d=350°C (Atom %)	(d) M=0.1 T_d=400°C (Atom %)
O	46.21	66.52	60.51	64.86
Si	16.80	00.00	00.00	00.00
Cl	12.24	00.00	02.74	00.00
Sn	24.75	33.48	36.76	35.14

AFM images are used for the investigation of SnO_2 surface topography (Figure 5). For all films, the 3D images present a rough surface with many bumps and valleys, which is in good agreement with the morphology observed by SEM and the structural crystallinity revealed by XRD spectra.

To study the nanoscale surface roughness, root mean square (RMS) is used. For 0.075 M films, the RMS values are evaluated at 427 nm, 122 nm for T_d=350°C and T_d=400°C, respectively. For 0.1 M films, RMS is equal to 195nm (T_d=350°C), and 116.2 nm (Td=400°C [2]). These results show that RMS values decrease significantly withthe increase of the deposition temperature T_d and the molarity M.

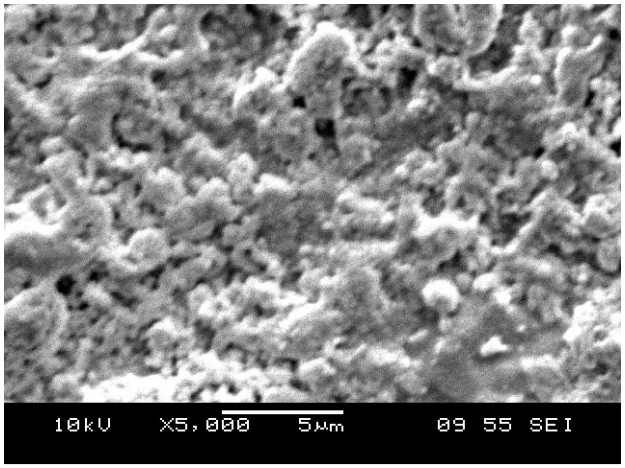

(a) M=0.075 Td=350°C.

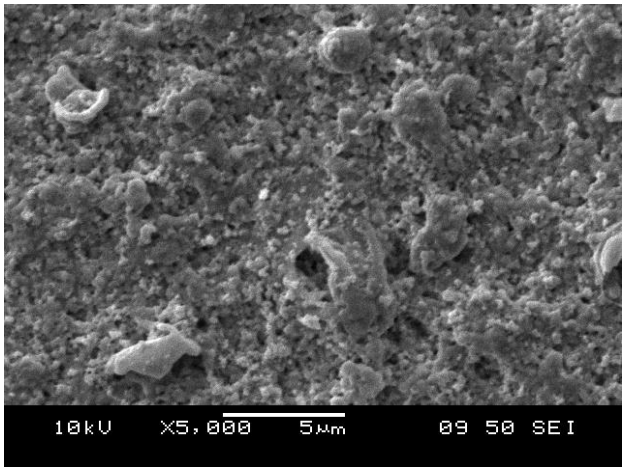

(b) M=0.075 T_d=400°C.

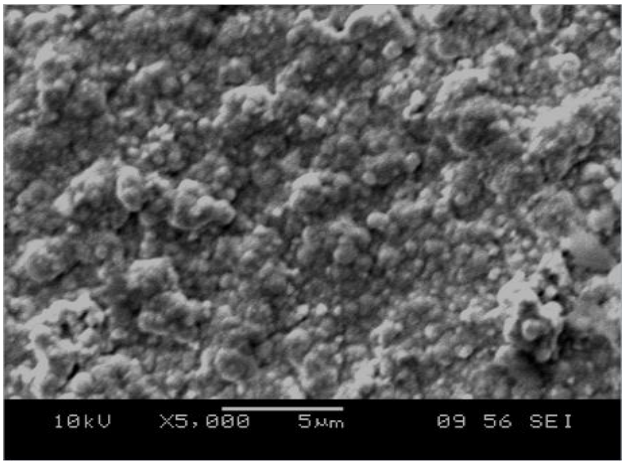

(c) M=0.1 Td=350°C.

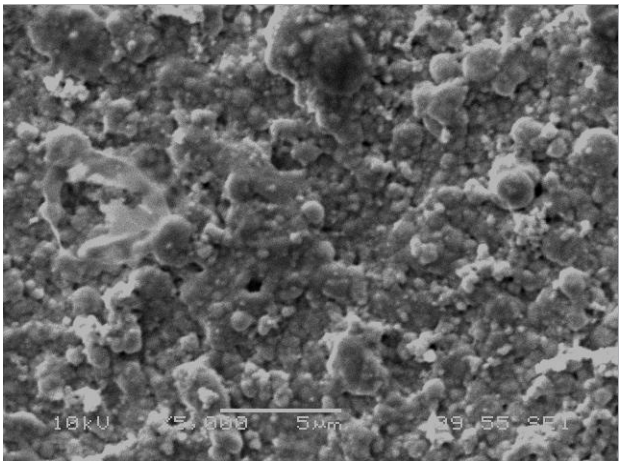

(d) M=0.1 T_d=400°C.

Figure 3. SEM micrographs of SnO_2 sprayed thin films.

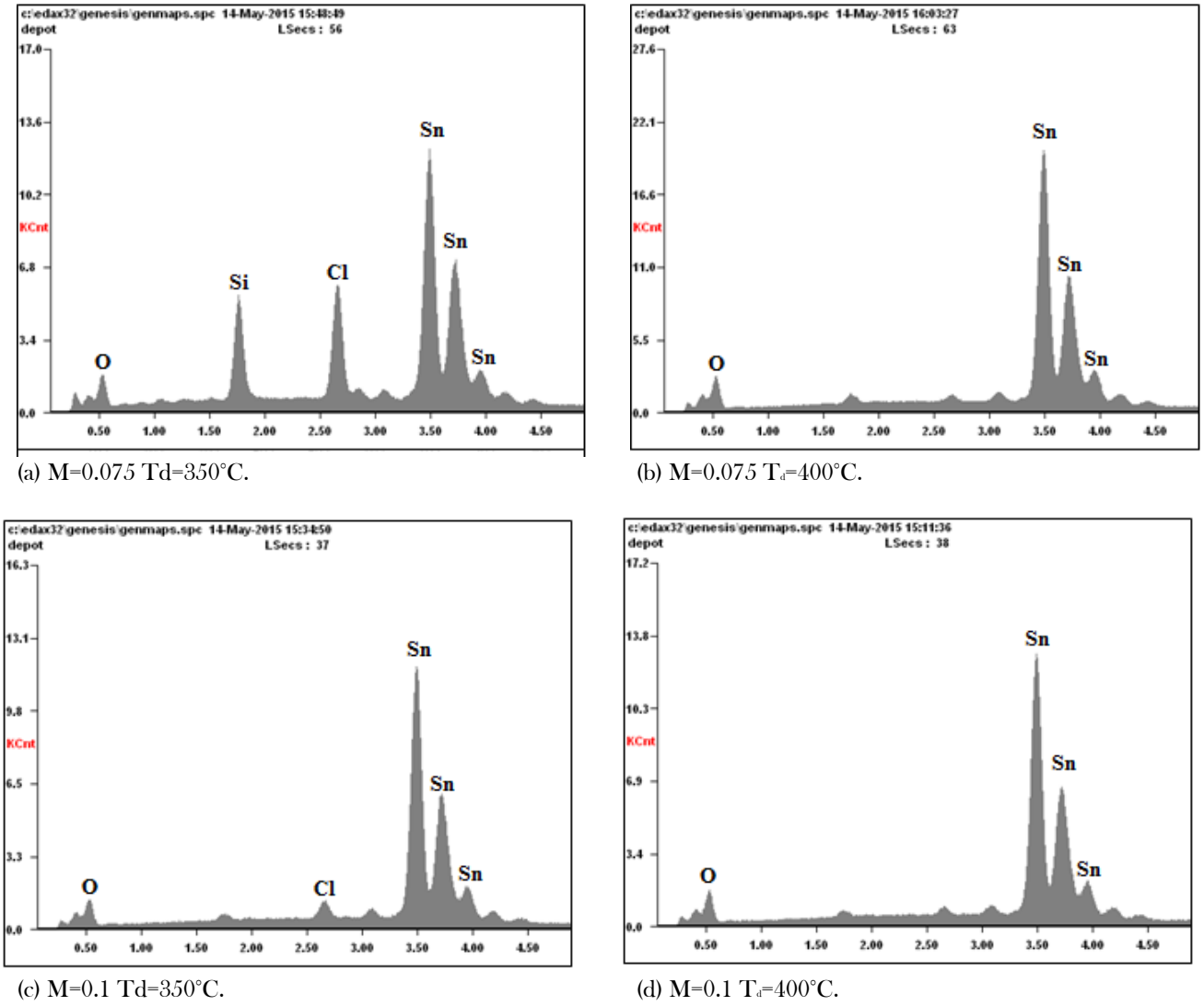

(a) M=0.075 Td=350°C. (b) M=0.075 T_d=400°C.

(c) M=0.1 Td=350°C. (d) M=0.1 T_d=400°C.

Figure 4. EDX elemental analysis of SnO_2 sprayed thin films.

Table 4: The values of the optical band gap energy (E_g) of SnO_2 thin films.

Samples deposition parameters	E_g [eV]
(a) M=0.075 T_d=350°C	3.03
(b) M=0.075 T_d=400°C	3.06
(c) M=0.1 T_d=350°C	3.07
(d) M=0.1 T_d=400°C	3.23

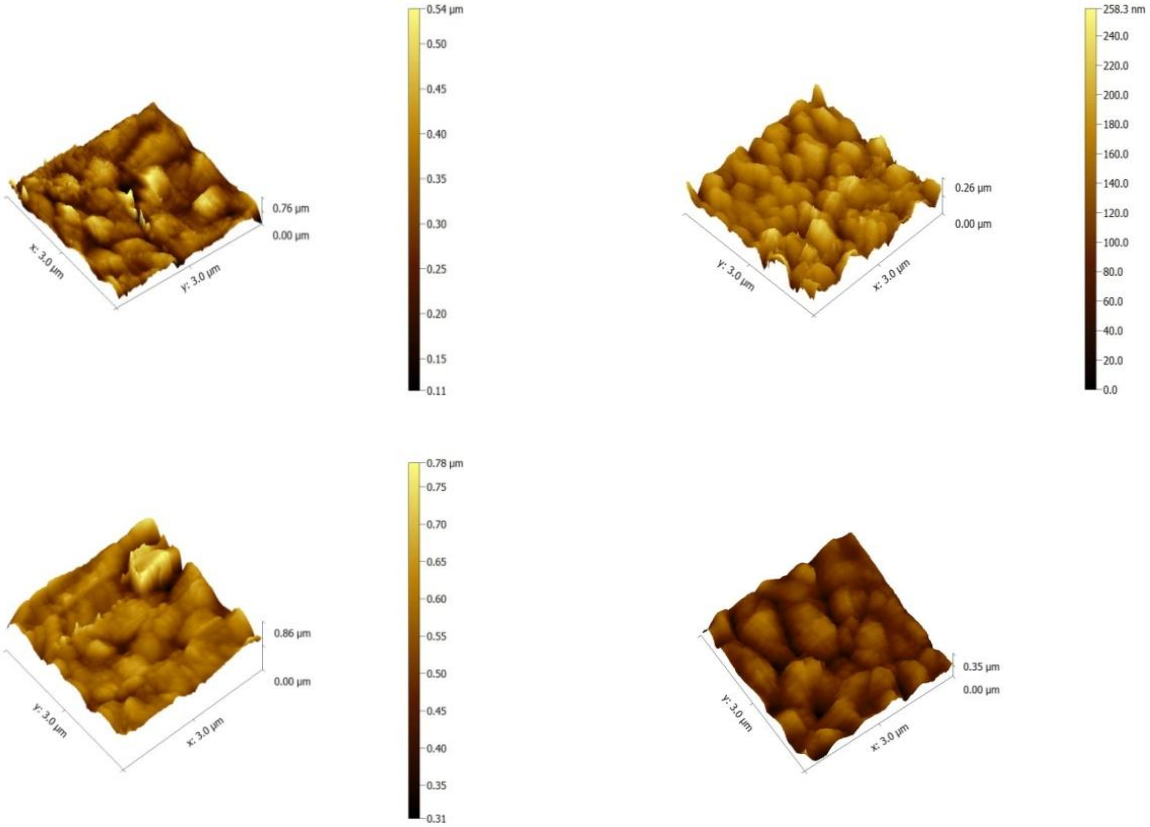

(a) M=0.075 Td=350°C.

(b) M=0.075 T_d=400°C.

(c) M=0.1 Td=350°C.

(d) M=0.1 T_d=400°C.

Figure 5. 3D AFM images of SnO_2 sprayed thin films.

3.3. Optical properties

The absorbance spectra of SnO_2 films are regrouped in Figure 6. The measurements were performed in the UV-visible-IR (200 nm - 1500 nm). The absorbance spectra decrease strongly from UV (5 % - 4.5 %) to the visible range (2.5 %-1 %). However, no significant decrease between the visible and IR regions is observed. In fact, we notice a gradual decrease in the visible region, then absorbance becomes almost constant in all infrared range. In Figure 7 we have plotted $(\alpha h\nu)^2$ vs. photon energy ($h\nu$). We have determined by linear extrapolation the values of the optical band gap E_g using Tauc's formula [23]:

$$(\alpha h\nu)^2 = B\,(E_g - h\nu)$$

Where α is the absorption coefficient, B a constant, h the Planck constant, Ethe energy band gap, and ν the incident photon frequency.

Optical band gap values are listed in Table 4, we notice a large band gap values that increase with the increase of the deposition temperature and molarity.

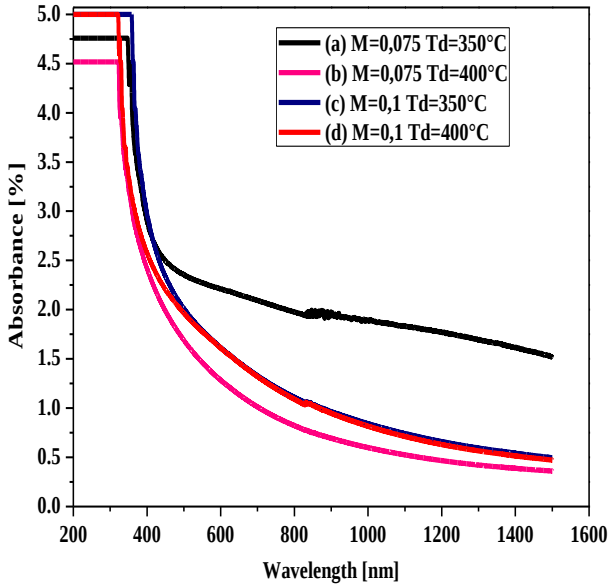

Figure 6. The absorbance spectra of SnO_2 sprayed thin films.

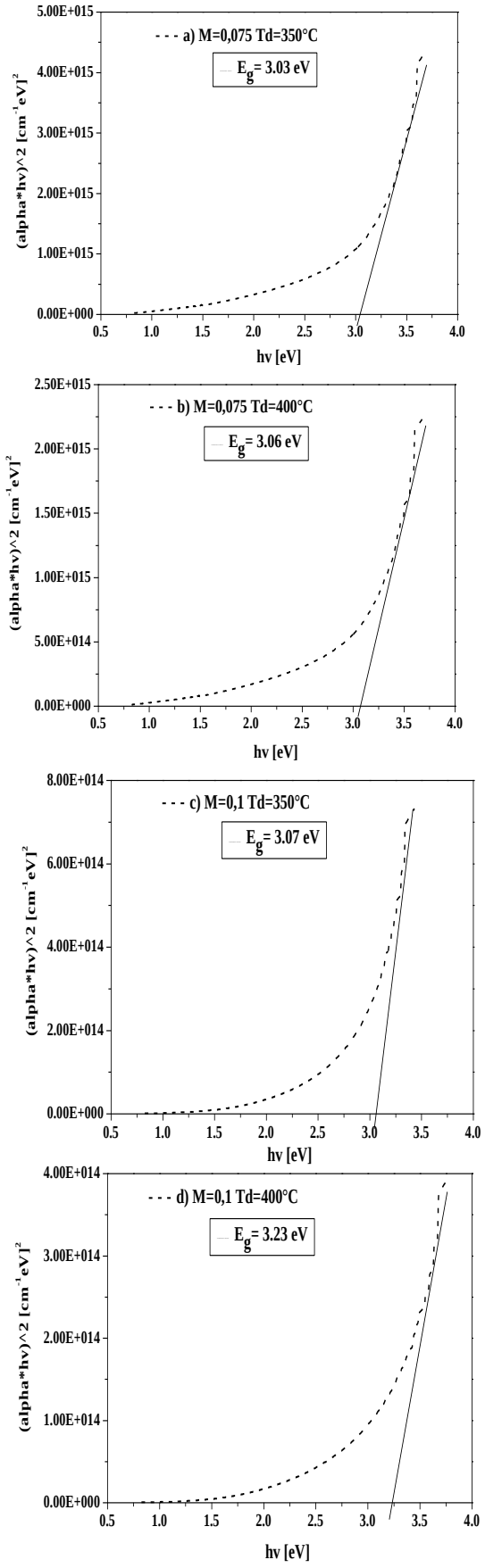

Figure 7. The Plot of $(\alpha hv)^2$ vs. hv of the SnO_2 sprayed thin films.

4. Conclusion

In this work, we have studied SnO_2 thin films deposited by spray pyrolysis at 350°C and 400°C using ($SnCl_2$, $2H_2O$) with two molarities (0.075 M and 0.1 M) in the aim to investigate their structural, morphological and optical properties. Structural properties by XRD showed that all SnO_2 deposited films are polycrystalline with a typical rutile tetragonal structure, except the T_d=350°C, 0.075 M film for which we observed a beginning of crystallization. All films have preferential growth along (110) plane and the crystallites sizes were estimated around 20 nm or less. SEM and AFM showed that surface morphology of the deposited layers is rough and porous with the presence of grains agglomerations of nanoparticles. EDX analysis confirmed the chemical composition and a good stoichiometry of SnO_2 deposited films. Moreover, higher RMS roughness was clearly observed at low molarity and deposited temperature. From optical properties, it was revealed that SnO_2 films present a large band gap values. All results obtained in this study from XRD, SEM, EDX and AFM are well correlated. The high crystallinity and roughness of the films let us conclude that the films may be well appropriate for interesting applications, especially in the biosensors field in the aim to study the improvement of their performances.

Acknowledgments

The authors would like to thank Dr. A.DJADOUN from Geophysics laboratory of USTHB University of Algiers, Algeria for the valued help in structural measurements. We are grateful to Prof. K.TAIBI from Crystallography and thermodynamics laboratory of USTHB University of Algiers for the contribution in SEM characterization. Also, we are thankful to Prof. M. ZAABAT from LCAM laboratory, Larbi ben M'hidi University of Oum el Bouaghi for his cooperation in AFM characterization.

References

[1] A.V. Singhal, K. Chandra, and V.Agarwala, Int. J. Nanotechnol. 12 (2015) 248.
[2] N.H. Touidjen, B. Bendahmane, M. Lamri Zeggar, F. Mansour and M.S. Aida, Sensing and Bio-Sensing Research. 11(2016) 52.
[3] S. Abbas, A. Ben Haoua, B. Ben Haoua, And A. Rahal, Journal of New Technology and Materials. 04 (2014) 106.
[4] J.P.Maranchi, A.F.Hepp, and P.N.Kumta, Materials Science and Engineering: B. 116 (2005) 327.
[5] M. Benhaliliba, Journal of New Technology and Materials. 05 (2015) 24.
[6] H.Howari, and I.B.I.Tomsah, Optik - International Journal for Light and Electron Optics. 144 (2017) 467.
[7] C. Ke, Z. Yang, W. Zhu, J. S. Pan, and S. Karamat, Journal of Applied Physics. 107 (2010) 88.
[8] A.V. Mudryi, A.V. Ivaniukovich and A.G. Ulyashin, Thin Solid Films. 515 (2007) 6489.

[9] Y. Liu, E. Koep, and M. Liu, Chem. Mater. 17 (2005) 3997.
[10] M. Khechbaa, A. Bouabellou, F. Hanini and S. Touati, Journal of New Technology and Materials. 02 (2017) 72.
[11] O. C. Monteiro, M. H. M. Mendonça, M. I. S. Pereira, and J. M. F. Nogueira, Journal of Solid State Electrochemistry 10 (2006) 41.
[12] J.B. Mooney, and S.B. Radding, Ann. Rev. Mater. Sci. 12 (1982) 81.
[13] P. Nunes, E. Fortunato, P. Vilarinho and R. Martins, State Phenomena. Vols. 80 (2001) 139.
[14] T. Serin, N. Serin, S. Karadeniz, H. Sarı, N. Tugluoglu, and O. Pakma, Journal of Non-Crystalline Solids. 352 (2006) 209.
[15] G. Gordillo, L. C. Moreno, W. de la Cruz, and P. Teheran, Thin Solid Films. 252 (1994) 61.
[16] Korotcenkov, G., V. Brinzari, J. Schwank, M. DiBattista and A. Vasiliev, Sensors and Actuators B. 77 (2001) 244.
[17] N. F. Habubi, Z. M. Abood, and A.N. Algamel, International Letters of Chemistry, Physics and Astronomy. 65 (2016) 80.
[18] A. A. Yadav, E. U. Masumdar, A. V. Moholkar, M. Neumann-Spallart, K. Y. Rajpure, and C. H. Bhosale, J. Alloys Compd. 488 (2009) 350.
[19] P. Scherrer, Göttinger Nachrichten Math. Phys. 2 (1918) 98.
[20] B. Thomas and B. Skariah, J. Alloys Compd. 625 (2015) 231.
[21] F. Paraguay-Delgado, M. Miki-Yoshida, W. Antunez, J. González-Hernández, Y.V. Vorobiev and E. Prokhorov, Thin Solid Films. 516 (2008) 1104.
[22] G. S. Park, and G. M. Yang, Thin Solid Films. 365 (2000) 7.
[23] J. Tauc, R. Grigorovici and A. Vancu, Phys.Status solidi B. 15 (1966) 627.